Wave Energy Resource Assessment around Kyushu based on Numerical Hindcast

Tomoaki Hirakawa
IGSES, Kyushu University

Abstract

To promote wave energy technologies, including wave energy converters (WECs), this study aims to present comprehensive analyses of wave climates around Kyushu. This paper calculates wave climate around Kyushu for 10 years (2007-2016) using the Simulating Waves Nearshore (SWAN) model with an approximately 800 m high spatial and 1-hour temporal resolution. Results reveal that the south side of Kyushu has more energetic waves than the north, and the southeast has the strongest energy among neighboring seas of Kyushu. In the southeast, the major portion of the wave energy transport is generated by extreme weather events. Wave climates in the southwest are less affected by extreme weather events, and the wave energy transport shows the opposite tendency to that of the southeast, suggesting that wave energy production in the southeast and southwest can supply high stable energy.

1. Introduction

While acknowledging the difficulty for renewables to take up nuclear energy's share in near future, the promotion of renewable energy technology is one of the key policies for Japan's stable future energy structure. In Japan, the first wave energy resource assessments were performed by Maeda and Kinoshita (1979)[1], stimulated by two oil crises. Maeda and Kinoshita (1979) calculated the distribution of mean wave energy transport $\bar{P}$ (kW/m) around Japan from 1954 to 1963. For Kyushu, the results showed that $\bar{P}$ = 11.57 in the east, ranging a latitude of 30°-35° and a longitude of 130°-135°, and $\bar{P}$ = 9.91 in the west, ranging a latitude of 30°- 35° and a longitude of 125°-130°. Maeda et al. (1981) [2] also obtained $\bar{P}$ = 12.7 for the east region and $\bar{P}$ = 11.0 for the west region from 1954 to 1963.

Tabata et al. (1980) [3] obtained P = 7.28 for southeast of Kyushu and P = 0.623 southwest of Kyushu for 1975 to 1978. Takahashi et al. (1989) [4] obtained $\bar{P}$ = 6.7 southeast of Kyushu and $\bar{P}$ = 1.6 southwest of Kyushu for 1970 to 1984. Directions and positions of $\bar{P}$ propagating from the southeast and southwest toward Kyushu described by Tabata et al. (1980) and Takahashi et al. (1989) are depicted in figure 1. Takahashi et al. (1989) also studied the joint distribution of $H_{1/3}$ and $T_{1/3}$ around Japan; however the wave direction and directional spectrum were not discussed. Recently, a wave energy assessment was performed for Japan between 1994 and 2014 using WaveWatchIII. The mean wave energy transport 30 km off Japanese coasts was estimated as $\bar{P}$ = 7.35. However, comprehensive analyses of waves around Kyushu were not discussed.

This study aims to present comprehensive analyses of statistics of wave characteristics around Kyushu using a high-resolution numerical model.

2. Data and Model

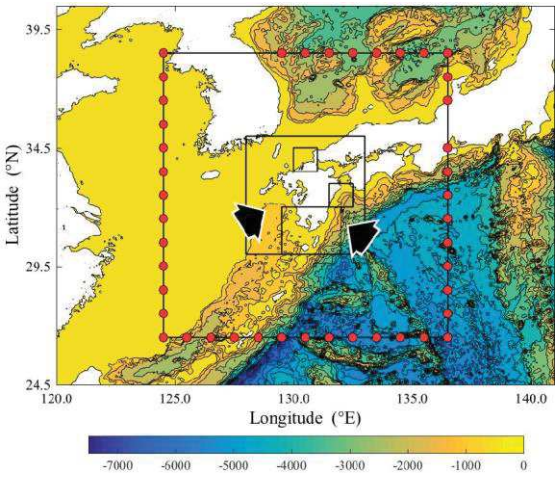

FIGURE 1. Five computational domains and bathymetry in Kyushu. Red dots describe NCEP data used for boundary conditions of SWAN's computation. Two arrows describe directions and positions of the mean wave energy transport $\bar{P}$ calculated by Tabata et al. (1980)[3] and Takahashi et al. (1989) [4] according to their papers.

The present study makes use of a third-generation wave model, Simulating Waves Nearshore (SWAN)[5, 6]. The basis of the formulation is the wave action balance equation:

$$\left(\frac{\partial}{\partial t}+c_x\frac{\partial}{\partial x}+c_y\frac{\partial}{\partial y}+c_\sigma\frac{\partial}{\partial \sigma}+c_\theta\frac{\partial}{\partial \theta}\right)N=\frac{\Sigma}{\sigma} \quad (1)$$

where N, defined as $N(x, y, t, \sigma, \theta) = S(x, y, t, \sigma, \theta)/\sigma$, is the action density, S is the directional wave energy density spectrum (hereinafter referred to as directional spectrum), θ is the direction, x and y are the horizontal coordinates, and t is time. σ is the relative wave frequency, defined as $\sigma = \omega$-$\mathbf{k}$ $\mathbf{u}$ where ω is the absolute wave frequency, $\mathbf{k}$ is the wave number vector, and $\mathbf{u}$ is the ambient current velocity vector. The Σ in (1) descries source terms. For inputs to SWAN, wind forcing was provided by JMA. Bathymetry data are provided from GEBCO 30 arc-second gridded data.

We used datasets containing significant wave heights, primary wave mean periods and primary wave directions for every three hours from WaveWatchIII data provided by the U.S. National Oceanic and Atmospheric Administration (NOAA). The red dots in figure 1 show locations from NOAA datasets that were taken for the boundary shown in the black square.

To calculate, computational domains with more detailed grid cells were nested in domains with coarser grid cells and received boundary conditions from results of coarser domains. Domain 1 is the largest of five domains. Domain 2, which is in domain 1, is the second largest and holds three smaller domains, designated domains 3, 4, and 5. Detailed descriptions of domains are shown in table 1.

Table 1: Setups of computational domains. The first number in each cell is regarding the longitude, and the other one is regarding latitude.

Domain name	Distance of sides (.)	Number of Grid cells	Distance of cells (m)
Domain 1	12.12	200.200	6000.6700
Domain 2	5.5	200.200	2400.2800
Domain 3	1.1	150.150	620.740
Domain 4	1.1	150.150	630.740
Domain 5	2.5.2	375.300	640.740

3. Result and discussions

3.1 Yearly and seasonal mean wave energy transport $\bar{P}$

The mean wave energy transport $\bar{P}$ is examined in this section. It is revealed that the south side of Kyushu possesses larger wave energy than the north side does, which was overlooked in previous studies due to the absence of measured data. Figure 2 shows $\bar{P}$ calculated for 10 years in domain 5, which was performed with the highest resolution in our computation (see table 1 for details).

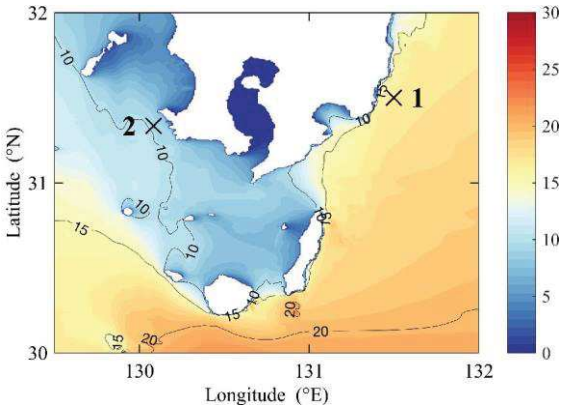

FIGURE 2. Spatial distribution of the mean wave energy transport $\bar{P}$ in domain 5 for 10 years.

In figure 2, contour line for $P = 15$ is close to the southeast coasts of the main island. These coasts have the most energetic waves around Kyushu. However, the energy of strong waves is mainly concentrated in the end of 05-07 and 08-10. We see this from figure 3. In 08-10, Kyushu is frequently struck by typhoons from the south tropical region; consequently, mean seasonal wave energy transport in 08-10 significantly increases up to approximately $\bar{P} = 30$ in the southeast.

Considering less extreme weather events from figure 3, we selected a site 10 km off the tip of the peninsula in the southwest, which is indicated by x2 in figure 2. Figure 2 shows that waves at x2 are expected to have a yearly mean wave energy transport of $\bar{P}$ 10. P at x2 is relatively constant and shows a completely different tendency to that at x1. In 05-07, wind from the northwest starts shifting to the southwest and south; consequently, P at x2 decreases and P accordingly increases for the southeast coast because the long fetch and duration in the Pacific.

The completely different tendencies between P in the southeast and southwest suggest that wave energy production in these regions can compensate for each other to supply high stable energy.

Statistical wave characteristics are important for estimating and improving wave energy production. In the next section, we analyze statistical wave characteristics at ،1 and ،2 using several useful plots.

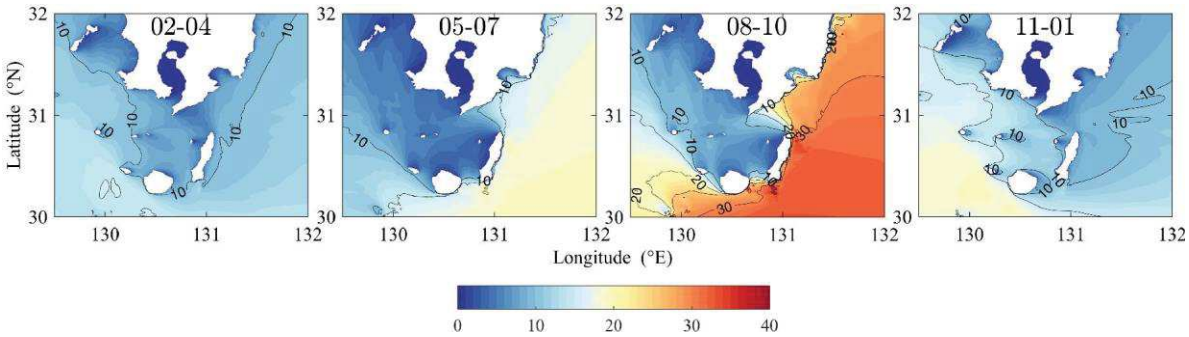

FIGURE 3. Seasonal spatial distributions of mean wave energy transport P calculated in domain 5 for (a) 11-01; (b) 02-04; (c) 05-07; and (d) 08-10. The wind fields are obtained from JMA and extrapolated by SWAN.

3.2 Wave characteristics

The water depths at x1 and x2 are 120 and 187 m, respectively; therefore only offshore WECs are suited for these sites. Considering the distance from the coasts regarding electrical power transmission, x1 and x2 are selected to be approximately 10 km off the coasts. At both x1 and x2, P can be approximated by the wave energy transport for deep water P_{deep}, assuming a linear narrow-band spectrum and deep water: P $P\text{deep} = \rho g^2 H^2_{m0} T_e/(64\pi)$, where T_e describes the period of wave energy, and we used $T_e = Tmm10$ in this study.

We studied the seasonal joint distribution and histograms of $Hm0$ versus $Tmm10$. At x1 in 02- 04 and 11-01, joint distributions resemble each other, having small mean significant wave height $\bar{Hm0}$ and period $\bar{Tmm10}$ (not shown here). In 05-07 to 08-10, as expected from figure 3. extreme weather events are apparent from large $Hm0$ and long $Tmm10$ (see figure for season 08-10). Peaks of the contour plot and histograms in 08-10 indicate that ($Tmm10$, $Hm0$) (8, 1) is the mode and more likely to occur, whereas the mean significant wave height and period are ($Tmm10$, $Hm0$) = (8.71, 1.86). The large difference between the mode and mean suggest that the mean values ($Tmm10$, $Hm0$) are strongly affected by extreme weather events.

Figure 5 shows means of seasonal directional spectra $\bar{S}(f, 0)$ at x1 and x2 in the season 08-10 and for 10 years: $\bar{S} = \frac{1}{M}\sum_{j=1}^{M} Sj$. In 02-04 and 11-01, $\bar{S}$ also resemble each other, both showing that the spectrum $S(0.46, 85)$ carries the largest energy (not shown here). In 05-07 and 08-10, large two peaks are broadly distributed in 0. Peaks in the direction 0 90 correspond to ordinary waves observed throughout the years, and the other peak in the direction 0 150 corresponds to extreme waves. There is little difference between frequencies f of ordinary waves and extreme waves. Figure 6 shows seasonal wave roses for the season 08-10 and x1 and x2 which are two-dimensional histograms consisting of $Hm0$ and the mean wave direction $0j$. The wave rose for 08-10 shows that extreme waves propagate in 0 140.

The relatively small seasonal variation in wave direction suggests that the use of WECs, depending upon wave direction, is possible in the southeast.

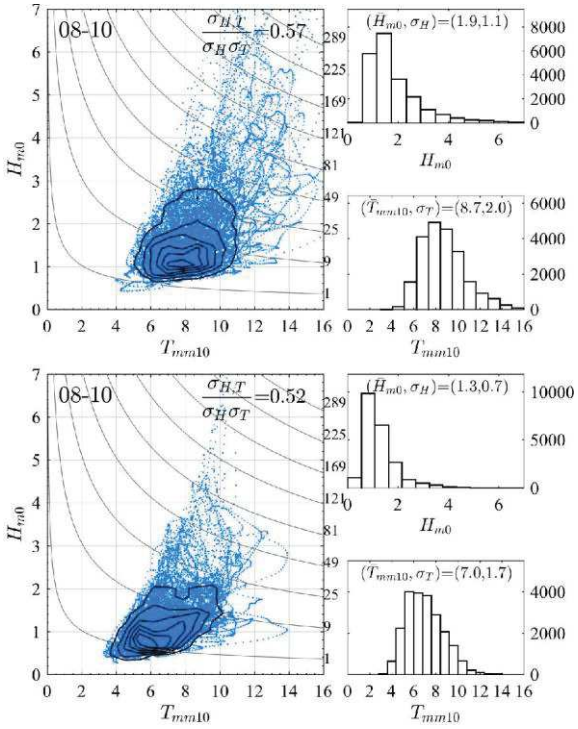

FIGURE 4. Joint distributions of ($Tmm10$, $Hm0$) and histograms of $Hm0$ and $Tmm10$ at 1 (top) and 2 (bottom) for 08-10. Contour lines in joint distributions show wave energy transports for deep water $\bar{P}$ (kW/m) of indicated on the values vertical axis at the right.

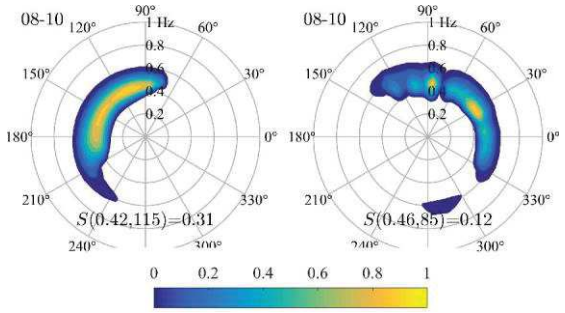

FIGURE 5. Normalized 10-years mean directional spectra $\bar{S}(f,9)$ at x1 (left) and x2 (right) for 08- 10. $\bar{S}(f, 9)$ are normalized with the maximum values described in each figure.

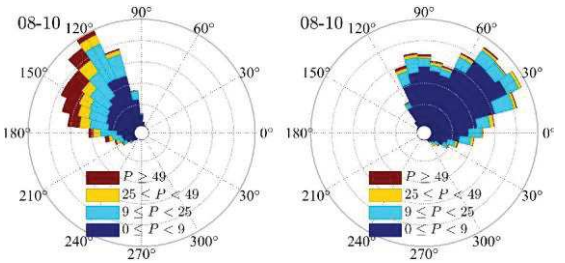

FIGURE 6. Wave roses of wave energy transport P at x1 (left) and x2 (right) for 10 years in 08-10.

At location x2, in 02-04 and 11-01, joint distributions of $Hm0$ and $Tm01$ are similar to each other, having larger $\bar{H}m0$ than seasons 05-07 and 08-10. Means of seasonal directional spectra at x2 in figure 5 show more peaks and marked seasonal variations in wave direction than those at x1. One of the peaks approximately at $\bar{S}(0.5, 30)$, is consistently observed in all seasons. In 05-07 and 08-10, peaks at $\bar{S}(0.4, 90)$ are thought to be caused by typhoons from the south, which is similar to the case in x1. In 11- 01 and 02-04, peaks at $\bar{S}(0.5, 350)$ are thought to be caused by monsoon from the continent (not shown here).

Seasonal wave roses at x2 also show marked seasonal variations in wave direction; accordingly, it is suggested that the use of WECs, without depending upon wave direction, is advantageous in the southwest.

4. Conclusion

The spatial distribution of the mean wave energy transport $\bar{P}$ for 10 years revealed that Kyushu has more wave energy in the south than in the north, which was overlooked in previous studies due to the absence of measured data. Mean wave energy transport $\bar{P}$ is highest in the southwest. The spatial distribution of $\bar{P}$ for 10 years showed wave energy up to $\bar{P}$ 16 in the southeast and P 10 in the southeast can be obtained if offshore waves are taken into consideration, which is greater than $\bar{P}$ estimated by Tabata et al. (1980) and Takahashi et al. (1989).

According to the spatial distribution of seasonal $\bar{P}$, extreme weather events frequently strike this region in 08-10. In 08-10, at x1 which is approximately 10 km off the coast, the monthly P and the ratio of monthly $\bar{P}$ relative to total yearly $\bar{P}$ are expected to reach $\bar{P}$ = 29 and 0.45, respectively. Although the yearly $\bar{P}$ is expected to be powerful on the southeast coast, a stable high-energy supply cannot be possible, and such extreme weather events may cause severe damage to WECs. P at x2 is relatively constant and shows the opposite tendency of P at x1. The opposite tendencies between P in the southeast and southwest suggest that if WECs can efficiently absorb wave energy including those of extreme waves, wave energy product southeast and southwest of Kyushu can compensate each other to supply high stable energy.

Statistical wave characteristics in the southeast and southwest represented by x1 and x2 also showed different tendencies in terms of seasonal wave direction variation.

The relatively small seasonal variation in wave direction at x1 suggests that the use of WECs, depending upon wave direction, is possible in the southeast, whereas marked seasonal variations in wave direction at x2 suggest that the use of WECs without depending upon the wave direction is advantageous southwest of Kyushu.

Reference

[1] H. Maeda and T. Kinoshita, "Wave Power Absorption," *Inst. Ind. Sci. Univ. Tokyo*, vol. 31, no. 11, pp. 1–10, 1979.
[2] H. Maeda, T. Kinoshita, and S. Kato, "Fundamental Research on Absorbing Energy from Ocean Waves (2nd report)," *J. Soc. Nav. Archit. Japan*, no. 149, pp. 65–72, 1981.
[3] T. Tabata, T. Yagyu, and I. Fukuda, "Wave Energy on Japanese Coast," *Rep. Port Harb. Res. Inst.*, no. 364, pp. 1–15, 1980.
[4] S. Takahashi and T. Adachi, "Wave Power around Japan from a Viewpoint of Its Utilization," *Rep. Port Harb. Res. Inst.*, no. 654, pp. 1–19, 1989.
[5] N. Booij, R. C. Ris, and L. H. Holthuijsen, "A Third-Generation Wave Model for Coastal Regions: 1. Model Description and Validation," *J. Geophys. Res.*, vol. 104, pp. 7649–7666, apr 1999.
[6] R. C. Ris, L. H. Holthuijsen, and N. Booij, "A Third-generation Wave Model for Coastal Regions: 2. Verification," *J. Geophys. Res.*, vol. 104, pp. 7667–7681, apr 1999.